TOXICOLOGICAL SCIENCES **132(1)**, 235–249 2013
doi:10.1093/toxsci/kfs325
Advance Access publication November 14, 2012

2,3,7,8-Tetrachlorodibenzo-*p*-dioxin-Mediated Production of Reactive Oxygen Species Is An Essential Step in the Mechanism of Action to Accelerate Human Keratinocyte Differentiation

Lawrence H. Kennedy,*[,1] Carrie Hayes Sutter†[,1] Sandra Leon Carrion,† Quynh T. Tran,† Sridevi Bodreddigari,† Elizabeth Kensicki,‡ Robert P. Mohney,‡ and Thomas R. Sutter*[,†,2]

*Department of Chemistry and †Department of Biological Sciences and the W. Harry Feinstone Center for Genomic Research, University of Memphis, Memphis, Tennessee 38152-3370; and ‡Metabolon, Inc., Durham, North Carolina 27713

[1]These authors contributed equally to this study and report.
[2]To whom correspondence should be addressed at Department of Biological Sciences, University of Memphis, 239 Ellington Hall, 3700 Walker Avenue, Memphis, TN 38152. Fax: (901) 678-2458. E-mail: tsutter@memphis.edu.

Received July 30, 2012; accepted November 8, 2012

Chloracne is commonly observed in humans exposed to 2,3,7,8-tetrachlorodibenzo-*p*-dioxin (TCDD); yet, the mechanism of toxicity is not well understood. Using normal human epidermal keratinocytes, we investigated the mechanism of TCDD-mediated enhancement of epidermal differentiation by integrating functional genomic, metabolomic, and biochemical analyses. TCDD increased the expression of 40% of the genes of the epidermal differentiation complex found on chromosome 1q21 and 75% of the genes required for *de novo* ceramide biosynthesis. Lipid analysis demonstrated that eight of the nine classes of ceramides were increased by TCDD, altering the ratio of ceramides to free fatty acids. TCDD decreased the expression of the glucose transporter, SLC2A1, and most of the glycolytic transcripts, followed by decreases in glycolytic intermediates, including pyruvate. NADH and Krebs cycle intermediates were decreased, whereas NAD^+ was increased. Mitochondrial glutathione (GSH) reductase activity and the GSH/glutathione disulfide ratio were decreased by TCDD, ultimately leading to mitochondrial dysfunction, characterized by decreased inner mitochondrial membrane potential and ATP production, and increased production of the reactive oxygen species (ROS), hydrogen peroxide. Aryl hydrocarbon receptor (AHR) antagonists blocked the response of many transcripts to TCDD, and the endpoints of decreased ATP production and differentiation, suggesting regulation by the AHR. Cotreatment of cells with chemical antioxidants or the enzyme catalase blocked the TCDD-mediated acceleration of keratinocyte cornified envelope formation, an endpoint of terminal differentiation. Thus, TCDD-mediated ROS production is a critical step in the mechanism of this chemical to accelerate keratinocyte differentiation.

Key Words: **2,3,7,8-tetrachlorodibenzo-*p*-dioxin; epidermal barrier; differentiation; reactive oxygen species; mitochondrial dysfunction; glycolysis; ceramide biosynthesis.**

The epidermis of terrestrial mammals is composed of several stratified layers forming the epidermal barrier that protects the animal against dehydration and transepithelial permeability of chemicals or infection by microbes. Keratinocytes are the major cell type of the epidermis. As these cells migrate outward from the basement membrane, they undergo terminal differentiation during which biochemical and structural changes take place, including flattening of their shape from the original cuboidal morphology, alterations in lipid metabolism and composition (Gray and Yardley, 1975; Lampe *et al.,* 1983), replacement of cell membranes by proteinaceous cornified envelopes (CEs), and loss of cellular organelles such as the nucleus and mitochondria (Candi *et al.,* 2005). These changes are tightly regulated, in part, through gene expression mechanisms and complex biochemistry.

The most common adverse effect in humans exposed to the environmental pollutant 2,3,7,8-tetrachlorodibenzo-*p*-dioxin (TCDD, dioxin) is an alteration of the skin, termed chloracne. The mechanism of this toxicity is not well understood, but TCDD causes an alteration in the differentiation and proliferation of the skin resulting in thickening of the interfollicular squamous epithelium, as well as metaplasia and hyperkeratinization of the ducts of the sebaceous gland, with comedone formation (Panteleyev and Bickers, 2006). We and others have demonstrated that TCDD alters keratinocyte terminal differentiation *in vitro* (Greenlee *et al.,* 1985; Loertscher *et al.,* 2001; Sutter *et al.,* 2009). In an *in vivo* model of epidermal barrier formation, TCDD accelerates the formation of the barrier *in utero* by 1 day, demonstrating that TCDD dramatically alters the epidermal permeability function of the skin during mouse development (Sutter *et al.,* 2011). TCDD binds to and activates a transcription factor, the aryl

hydrocarbon receptor (AHR), causing its dimerization with the AHR nuclear translocator (ARNT). The AHR/ARNT heterodimer regulates the transcription of numerous genes via direct and indirect mechanisms.

Submerged cultures of early passage normal human epidermal keratinocytes (NHEKs) retain many of the regulatory, structural, and biochemical components of normal differentiation. Studies have shown that confluent cell density controls keratinocyte commitment to terminal differentiation and differentiated gene expression (List *et al.,* 2007; Paragh *et al.,* 2010; Sutter *et al.,* 2009; Tran *et al.,* 2012). We recently reported that TCDD alters the expression of genes involved in later aspects of keratinocyte differentiation, including genes involved in CE and lipid matrix biosynthesis (Sutter *et al.,* 2009). In a subsequent study, we reported on the direct transcriptional regulation of the human filaggrin (FLG) gene via the binding of the TCDD-activated AHR to the xenobiotic response elements found in the promoter of FLG (Sutter *et al.,* 2011). FLG aggregates keratin into filaments, which stabilize a network of structural proteins. Although the proper expression of FLG is critical to maintaining a normal skin phenotype, FLG is just one of the many genes located in the epidermal differentiation complex (EDC) of human chromosome 1q21 whose expression is elevated in response to exposure to TCDD (Sutter *et al.,* 2011). Here, we report the integration of genomic, metabolomic, and biochemical data that elaborate the biochemical effects of TCDD to affect keratinocyte differentiation. Moreover, these studies identify TCDD-mediated production of hydrogen peroxide (H_2O_2) as an essential step in the mechanism of TCDD to accelerate keratinocyte differentiation.

MATERIALS AND METHODS

Cell culture. Fifth-passage neonatal foreskin NHEKs (Lonza, Walkersville, MD) were grown as previously described (Sutter *et al.,* 2009, 2011). Briefly, cells were grown in keratinocyte serum–free medium (KSFM) (Invitrogen, Grand Island, NY) supplemented with 5 ng/ml epidermal growth factor and 50 μg/ml bovine pituitary extract. NHEKs were grown to confluence before pretreatment in KSFM for 24 h, followed by treatment in KSFM containing the control vehicle (0.1% dimethylsulfoxide) or 10nM TCDD for the indicated times. For AHR antagonists experiments, cells were grown to confluence and pretreated with α-naphthoflavone (ANF, 1μM, Sigma-Aldrich, St Louis, MO), or CH223191 (1μM, Sigma-Aldrich) for 1 h before treatment with TCDD (10nM), ANF, or CH223191 for the indicated times.

RNA isolation, quantitative real-time PCR, and microarray. For all RNA studies, cells were treated for 24 h. Total RNA isolation and quantitative real-time PCR (qRT-PCR) were performed as previously described (Sutter *et al.,* 2009) using the Pfaffl method (Pfaffl, 2001). Samples were normalized to values of tubulin, alpha 1C. Primers used in this study are listed in Supplemental Table S1. Affymetrix microarray data ($n = 4$ per sample group) was processed and analyzed as previously described (Tran *et al.,* 2012). A fold-change (FC) cutoff value of 1.25 was selected, and multiple hypothesis testing was corrected by Benjamini-Hochberg false discovery rate control at the 0.01 level (Benjamini and Hochberg, 1995), with an adjusted p-value of < 0.0023. The data have been submitted to the National Center for Biotechnology Information Gene Expression Omnibus repository (GSE36796). The bioinformatics tools used in this study were GeneIndexer (Homayouni *et al.,* 2005), DAVID (http://david.abcc.ncifcrf.gov/) for gene ontology and Kyoto Encyclopedia of Genes and Genomes (KEGG) analyses, Ingenuity Pathway Analysis (IPA, Ingenuity Systems, www.ingenuity.com), and PubMed (http://www.ncbi.nlm.nih.gov/pubmed/). The statistical analyses reported in the other figures were performed using GraphPad Prism 5.0, unpaired t-test ($p < 0.05$), or two-way ANOVA with Bonferroni's *post hoc* tests ($p < 0.05$). ImageJ was used for image quantitation (Abramoff *et al.,* 2004).

Lipid extraction and high-performance thin-layer chromatography. NHEKs were grown to confluence and treated in KSFM supplemented with 10μM linoleic acid (Sigma-Aldrich) for 24, 48, 72, or 96 h. Each sample contained ~2×10^7 cells. Lipids were extracted and analyzed as previously described (Tran *et al.,* 2012). The total lipid development system followed published work (Ponec and Weerheim, 1990).

Inner mitochondrial membrane potential assay. NHEKs were grown to confluence in 96-well fluorescent microplates (Corning, Salt Lake City, UT) and treated for 24, 48, or 72 h. Cells were washed with PBS. Following the wash, 100 μl of PBS containing 100μM 2-(4-dimethylamino)styryl-N-ethylpyridinium iodide (DASPEI) (Sigma-Aldrich), a mitochondrial potentiometric probe, and 25μM Hoechst 33342 (Sigma-Aldrich), a fluorescent nuclear dye, were added to each well and the microplates were incubated for 30 min at 37°C. Fluorescence was then measured using 485 ex/555 em for DASPEI and 320 ex/460 em for Hoechst 33342, with the relative fluorescent units used to normalize for cell number. Positive control cells were treated with carbonyl cyanide *m*-chlorophenyl hydrazone (Sigma-Aldrich, 100μM, 30 min) in order to depolarize the inner mitochondrial membrane (IMM).

Intracellular ATP concentration. NHEKs were grown to confluence and treated for 24, 48, or 72 h. Each sample contained ~2×10^6 cells. ATP was measured by chemiluminescence (CL) using an ATP Determination Kit (Life Technologies, Grand Island, NY), following the manufacturer's instructions, and a Turner Model 20/20 Luminometer (Promega, Madison, WI). Cells were washed with PBS, followed by collection in ATP-releasing buffer (100mM potassium phosphate buffer, pH 7.8, 2mM EDTA, 1mM dithiothreitol, 1% Triton X-100). Samples were centrifuged at 10,000 × g for 10 min. ATP was measured using 0.5 μg of protein and ATP standards. Protein concentrations were determined using the Bradford assay (Bio-Rad, Hercules, CA).

Mitochondrial glutathione, glutathione disulfide, and glutathione reductase activity assays. NHEKs were grown to confluence and treated for 72 h. Each sample contained ~2×10^7 cells. Mitochondrial pellets were isolated as described (Senft *et al.,* 2002a). Briefly, cell pellets were homogenized in ice-cold isolation buffer (70mM sucrose, 220mM mannitol, 2mM EDTA, 2mM ethylene glycol tetraacetic acid, and 2mM 4-(2-hydroxyethyl)-1-piperazineethanesulfonic acid (HEPES), pH 7.4, plus 1:500 vol/vol protease inhibitor cocktail (Sigma-Aldrich) using a motor-driven Potter-Elvehjem homogenizer (Bellco, Vineland, NJ) and a 12-mm Teflon pestle. The homogenates were placed in a centrifuge for 10 min at 1000 × g, and the supernatant fractions were spun a second time for 10 min at 1000 × g. The resulting supernatant suspensions were placed in a centrifuge for 15 min at 10,000 × g. The mitochondrial pellets were washed and then suspended in respiratory buffer (70mM sucrose, 220mM mannitol, 0.5mM EDTA, 2.5mM KH_2PO_4, 2.5mM $MgCl_2$, 0.1% bovine serum albumin, and 2mM HEPES, pH 7.4). Protein concentrations were determined using the Bradford assay (Bio-Rad). For determination of mitochondrial glutathione (GSH) and glutathione disulfide (GSSG), the mitochondrial suspensions were filtered through a 0.45-mm syringe-driven filter (Millipore Corp., Bedford, MA), yielding a 5% deproteinized homogenate. GSH and GSSG were determined spectrofluorometrically (Cary Varian Eclipse, Agilent Technologies, Santa Clara, CA) using the *o*-phthalaldehyde method as described (Senft *et al.,* 2000). For measurement of mitochondrial glutathione reductase (GSR) activity, the mitochondrial suspensions were sonicated using the Misonix Ultrasonic Processor XL (Farmingdale, NY) with the 419 standard tapered microtip at a power setting of 3 for 4 s. Activity was

measured as a function of the reduction in the absorbance of NADPH at 340 nm using a Glutathione Reductase Assay Kit (Sigma-Aldrich).

Mitochondrial H_2O_2 assay. NHEKs were grown to confluence and treated for 72 h. Each sample contained ~2 × 10^7 cells. Mitochondrial pellets were isolated as follows: Cell pellets were washed in wash buffer (134mM NaCl, 5mM KCl, 0.7mM Na_2HPO_4, 2.5mM Tris, pH 7.5) and resuspended in 10 volumes of swelling buffer (10mM NaCl, 1.5mM $CaCl_2$, 10mM Tris, pH 7.5, plus 1:500 vol/vol protease inhibitor cocktail [Sigma-Aldrich]) and incubated on ice for 15 min before they were homogenized using a motor-driven Potter-Elvehjem homogenizer and a 12-mm Teflon pestle. Immediately following lysis, sucrose (1.65M) was added to one fifth the total volume of the homogenates followed by centrifugation for 10 min at 1000 × g. The supernatants were placed in a centrifuge again for 10 min at 1000 × g. The resulting supernatants were placed in a centrifuge for 15 min at 10,000 × g, producing mitochondrial pellets. The pellets were washed twice in sucrose (0.35M) and resuspended in respiratory buffer (140mM KCl, 0.1mM EDTA, 2.5mM KH_2PO_4, 2.5mM $MgCl_2$, 0.05% bovine serum albumin, and 5mM HEPES, pH 7.4). H_2O_2 production was monitored as luminol (5-amino-2-3-dihydro-1,4-phthalazinedione) CL using a Turner Model 20/20 luminometer (Shertzer *et al.,* 2006). The reaction mixtures consisted of 5μM luminol, 2.5 U/ml horseradish peroxidase, 50 μg mitochondrial protein, and respiratory buffer to a final volume of 1.0 ml. One hundred microliters of 6 mM sodium succinate were added to initiate the reaction. Measurements were taken following 20 min incubation at 37°C, after determining that 20 min was within the linear range of the assay.

Metabolomics study. NHEKs were grown to confluence and treated in KSFM supplemented with 10μM linoleic acid for 24, 48, or 72 h. Each sample contained ~2 × 10^7 cells. Cells were washed with 8 ml of PBS, scraped into 15 ml tubes, centrifuged twice for 10 min at 500 × g, removing the supernatant each time. Pellets were flash frozen in a dry ice/ethanol slurry and stored at −80°C until their analysis. The metabolites were extracted using an automated MicroLab STAR system (Hamilton Co., Salt Lake City, UT). Cell pellets were suspended in 175 μl of water. From this suspension, 100 μl was taken for extraction, mixed with 450 μl of methanol containing recovery standards (fluorophenylglycine, tridecanoic acid, and cholesterol-*d*6), and shaken for 2 min at 675 strokes/min on a Geno Grinder 2000 (Glen Mills Inc., Clifton, NJ). The extracts were centrifuged for 5 min at 1000 × g. The supernatants were divided into aliquots for liquid chromatography-mass spectrometry (MS)/MS and liquid chromatography-MS (GC-MS) analyses. Quality control standards were added prior to analysis to monitor injection, chromatographic, and instrument reproducibility.

The ultraperformance liquid chromatography (UPLC) MS/MS platform utilized a Waters Acquity UPLC and a ThermoFisher LTQ mass spectrometer, which included an electrospray ionization source and a linear ion-trap mass analyzer (Evans *et al.,* 2009). The instrument was set to monitor for positive ions in acidic extracts or negative ions in basic extracts through independent injections. The instrument was set to scan 99–1000 m/z and alternated between MS and MS/MS scans. The scan speed was ~6 scans/s (three MS and three MS/MS scans). MS/MS scans were collected using dynamic exclusion, a process in which after a MS/MS scan of a specific m/z has been obtained, the m/z is placed on a temporary MS/MS exclude list for a user-set period of time to allow greater MS/MS coverage of ions present in the MS scan. This occurs because the instrument will not trigger an MS/MS scan of the same ion repeatedly. Extracts were loaded onto columns (Waters UPLC BEH C18-21 × 100 mm, 1.7 μm) and gradient eluted with water and 95% methanol containing 0.1% formic acid (acidic extracts) or 6.5mM ammonium bicarbonate (basic extracts). Columns were washed and reconditioned after each injection.

The samples for analysis by GC-MS were dried under vacuum desiccation prior to being derivatized under dried nitrogen using bistrimethyl-silyl-trifluoroacetamide. Derivatized samples were separated on a 5% phenyldimethyl silicone column with helium as the carrier gas and a temperature ramp from 60°C to 340°C within a 17-min period. All samples were analyzed on a Thermo-Finnigan Trace DSQ MS operated at unit mass resolving power with electron impact ionization and an atomic mass unit scan range of 50–750.

Metabolites were identified by automated comparisons to entries in Metabolon's proprietary library. A combination of mass spectral and chromatographic properties was used to assign an identity to specific biochemicals. The identification of named chemical entities was based on a comparison to the internal metabolomic library entries of purified standards which were run on the same analytical platform (Dehaven *et al.,* 2010). For data and statistical analyses, the relative quantification was derived from raw detector counts for the mass spectrometers. Following data extraction, automated quality control checks, and curation (confirming that biochemicals were correctly identified by the automated software), data were presented as a series of peak area quantities. Raw area counts for a biochemical were divided by the median value for that biochemical across all treatments, setting the medians equal. Data were normalized using protein content as determined by the Bradford assay (Bio-Rad). Statistical analysis of data was performed using JMP (SAS, http://www.jmp.com) and "R" (http://cran.r-project.org/), a freely available, open-source software package. Two-way ANOVA, followed by a Welch's two-sample *t*-test, was performed on the full factorial design of treatment and time. A log transformation was applied to the observed relative concentrations for each biochemical because, in general, the variance increased as a function of the average response of a given biochemical and because ratios were being compared. Those biochemicals with detectable levels in a majority of the samples were included in the analyses. Missing values were assumed to be below the limit of detection and were imputed with the minimum for that biochemical across all groups. Welch's two-sample *t*-tests were used to compare each dose to the control group, at each time point evaluated.

CE competence assay. NHEKs were grown to confluence and treated in medium supplemented with 1.8mM Ca^{2+} for 72 h in the presence or absence of an antioxidant: N,N′-diphenyl-*p*-phenylenediamine (DPPD, 2.5μM, Sigma-Aldrich), quercetin (10μM, Sigma-Aldrich), N-acetyl-L-cysteine (NAC, 1.25mM, GNC), catalase (500 U/ml, Sigma-Aldrich), or polyethylene glycol–conjugated catalase (PEG-catalase, 1000 U/ml, Sigma-Aldrich). The CE competence assay was performed as described (Tran *et al.,* 2012). The percentage of CEs was calculated as the ratio of CEs to total cell count.

RESULTS

The Effects of TCDD on NHEK Gene Expression

Treatment of NHEKs with 10nM TCDD for 24 h significantly altered the expression of 3300 genes that were divided into two lists: increased and decreased in response to TCDD. Gene ontology analysis identified "Epidermal Differentiation" as the top functional annotation cluster enriched (*p*-value, 5.3E−13) by genes whose expression was increased by TCDD, and "Mitochondrion" as the top cluster enriched (*p*-value, 3.9E−34) by genes whose expression was decreased by TCDD.

TCDD Increases the Expression of Genes Required for Cornified Envelope Formation

As part of its effect to accelerate epidermal differentiation (Greenlee *et al.,* 1985; Loertscher *et al.,* 2001; Sutter *et al.,* 2009), TCDD significantly increased the expression of 24 of the 60 genes of the EDC found on human chromosome 1q21 (Fig. 1A). This complex encodes four major classes of proteins involved in cornified envelope formation: the late cornified envelope (LCE) proteins, the small proline-rich proteins (SPRRs), the filaggrin proteins (FLG), and the calcium-binding S100A proteins. TCDD also increased the levels of RNA of more than 200 additional genes that contribute to epidermal

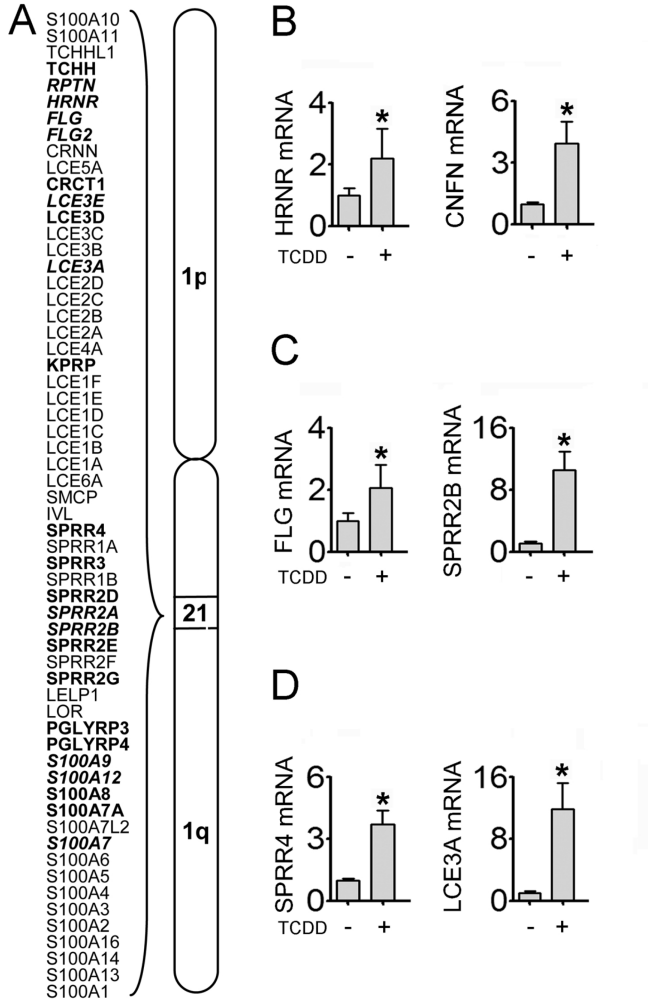

FIG. 1. TCDD modulates the expression of genes critical to the formation of the cornified layer. (A) Depiction of the microarray analysis of the EDC, located on human chromosome 1q21, following treatment with TCDD. The level of RNA corresponding to the genes in bold print (normal and italics) had increased expression in response to TCDD (24 h). The genes in italic bold print confirmed previously published increases in expression (Sutter *et al.,* 2011). The RNAs of the remaining genes were not significantly altered by TCDD. (B)–(D) qRT-PCR was used to verify the FC values obtained in microarray analysis for the indicated genes following TCDD treatment (24 h). Levels of RNA (mean [$n = 4$] ± SD) are expressed in units relative to the DMSO control, given a value of 1. *$p < 0.05$ indicates a significant difference between the control and treated samples.

differentiation, yet are not located in the EDC (Supplementary table S2). Figure 1B shows examples of the effects of TCDD, validated by qRT-PCR, of the EDC-encoded gene hornerin (HRNR), and cornifelin (CNFN), located on chromosome 19, encoding a protein which is found crosslinked with the major CE proteins loricrin and involucrin (Michibata *et al.,* 2004). The levels of each of these RNAs were increased by approximately three- to fourfold in response to treatment by TCDD. However, the effect of TCDD on the expression of other genes was not always proportional. For example, the expression of FLG was increased twofold by TCDD (Fig. 1C, left), whereas the expression of SPRR2B was increased 10-fold in response to TCDD (Fig. 1C, right). Such changes in the relative expression levels of these RNAs are indicative of alterations in the stoichiometry of these CE constituents. Additionally, TCDD increased the expression of several genes not normally associated with keratinocyte differentiation, yet known to be abnormally elevated in inflammatory skin diseases such as psoriasis or atopic dermatitis (Supplementary table S3). For example, RNA levels of the SPRR4 and late cornified envelope 3A (LCE3A) are increased by TCDD (Fig. 1D). Analysis of the literature identified 84 TCDD-responsive genes that are associated with diseases of the skin. Sixty-nine percent of these genes (58 genes) were associated with psoriasis, whereas 18% were associated with atopic dermatitis (Supplementary table S3). Of the psoriasis-related genes, 30% (17 genes) are known to have genetic mutations, whereas 69% (40 genes) are known to have altered levels of expression in the diseased skin. Remarkably, for 87% of the 40 genes having altered expression in psoriasis, the direction of the change in expression (up or down) in response to TCDD was the same as reported in psoriasis.

TCDD Alters Ceramide Biosynthesis

The lipid matrix of the stratum corneum is primarily composed of cholesterol, free fatty acids (FFA), and ceramides (Cer), with Cer being the dominant species by weight (Uchida and Holleran, 2008). TCDD increased the expression of three of the four genes encoding enzymes in the *de novo* pathway for Cer synthesis, including the rate-limiting enzyme, serine palmitoyltransferase (Perry *et al.,* 2000), ceramide synthase 3 (LASS3), and degenerative spermatocyte homolog 2 (DEGS2) (Fig. 2A). Cer synthesis occurs in the endoplasmic reticulum. Following synthesis, Cer are transported to the Golgi where UDP-glucose ceramide glucosyltransferase (UGCG) and sphingomyelin synthase (SGMS) add glucose and choline phosphate functional groups, producing glucosylceramide (GCer) and sphingomyelin, respectively. These two lipid classes are transported into lamellar bodies and are the precursors of the Cer present in the lipid matrix of the cornified layer. TCDD increased RNA expression of UGCG 1.9-fold, as well as increased RNA expression of glucosylceramidase (GBA) 2.4-fold. GBA encodes the enzyme that cleaves the beta-glucosidic linkage following extrusion from the cell (Hamanaka *et al.,* 2002). Likewise, TCDD increased the expression of sphingomyelin phosphodiesterase 3 (SMPD3) 1.9-fold. SMPD3 converts sphingomyelin back to Cer following extrusion (Uchida and Holleran, 2008). The microarray results for the RNAs of this pathway were validated by qRT-PCR (Supplementary fig. S1A). These results indicate an overall upregulation in Cer biosynthesis and would predict an increase of Cer in response to TCDD.

To investigate whether changes in gene expression resulted in alteration in the composition of lipids in differentiating

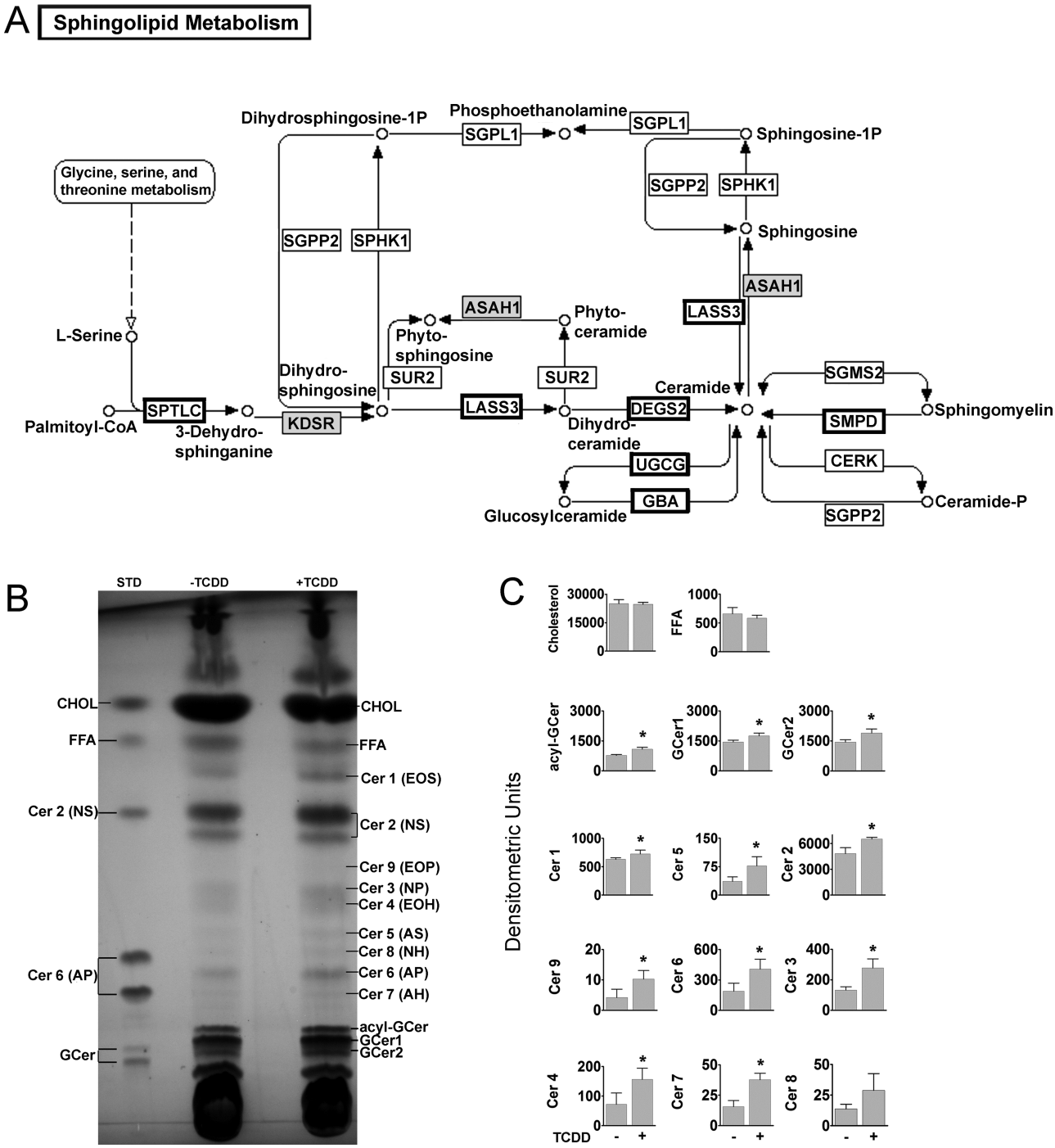

FIG. 2. TCDD enhances sphingolipid biosynthesis in NHEKs. (A) The sphingolipid metabolism pathway adapted from the KEGG pathway database. Bold outlined boxes indicate RNAs significantly increased, and gray boxes indicate RNAs significantly decreased, in response to TCDD (24 h) based on microarray analysis. Note: DEGS2 and LASS3 were significant by qRT-PCR analysis, but not in the analysis of the microarray data. (B) A representative HPTLC plate using a ceramide development system of lipid extracts from control or TCDD-treated cultures of NHEKs (72 h). (C) Quantitation using densitometry of the indicated lipid bands (mean [$n = 3$] ± SD). *$p < 0.05$ indicates a significant difference between the control and treated samples.

NHEKs, lipids were extracted and separated by high-performance thin-layer chromatography (HPTLC). A time course experiment showed that the greatest difference in Cer 2 and GCer between control and TCDD-treated cells occurred at 72 h (Supplementary fig. S1B). Acyl-GCer and three of the four GCer, that are the precursors of the Cers in the lipid matrix, were increased by TCDD treatment (Supplementary fig. S1C and D). Likewise, eight of the nine Cer classes known to be

present in the skin (Breiden *et al.,* 2007) were increased by TCDD (Figs. 2B and C). Taken together, these data indicate that TCDD affects the expression of Cer biosynthetic genes and results in increased levels of acyl-GCer, GcCer, and Cer in differentiating NHEKs, without altering the levels of cholesterol or FFA.

TCDD Impairs Mitochondrial Function in NHEKs

TCDD changes the RNA expression of many nuclear-encoded mitochondrial genes that have direct impact on mitochondrial function (Fig. 3A). Specifically, within complex 1 of the electron transfer chain (ETC), TCDD decreased the expression of several structural subunits: NDUFS1, NDUFS2, NDUFS3, NDUFA8, NDUFA12, NDUFB5, and NDUFC1, 1.4-, 1.4-, 1.6-, 1.5-, 2.7-, 1.6-, and 1.5-fold, respectively. Within complex 2, the catalytic subunits SDHC and SDHD were both decreased 1.5-fold. Within complex 3, the structural and proton-pumping subunits, UQCRFS1 and UQCRB, were decreased 1.3- and 1.4-fold, respectively. Within complex 4, several regulatory and structural subunits were affected by TCDD. Specifically, TCDD increased the expression of COX7B 1.9-fold and decreased the expression of COX7A2L, COX11, and COX15, 1.4-, 1.5-, and 1.3-fold, respectively. Finally, within complex 5, TCDD altered the expression of several proton transporting subunits: TCDD increased the expression of ATP6V1B2, ATP6V1E1, ATP6V1G1, and ATP6V0C, 1.3-, 1.4-, 1.7-, and 1.3-fold, respectively, and decreased the expression of ATP5A1, ATP5C1, ATP6V1C1, and ATP6V0E1, 1.4-fold each (Supplementary table S4). Given the large number of nuclear-encoded mitochondrial genes affected by TCDD, and the inherent difficulty of measuring their functions independently, we assessed mitochondrial function by measuring IMM potential and ATP production. By 48 h of treatment, TCDD significantly reduced IMM potential (Fig. 3B) and ATP production (Fig. 3C); these effects were more pronounced at 72 h, showing a 30% reduction in IMM potential and a 40% decrease in ATP production. Loss of IMM potential is known to be a marker of mitochondrial dysfunction (Crompton, 1999), and ATP production is the ultimate measure of electron transport chain (ETC) effectiveness. To assess whether the effects of TCDD on nuclear encoded mitochondrial gene expression and ATP production may be AHR mediated, studies using the AHR antagonists, ANF, and CH223191, were performed. TCDD-mediated repression of NDUFS1 and NDUFS3, each encoding core subunits of mitochondrial complex I, was abolished by cotreatment with either AHR antagonist (Supplementary fig. S2). Similarly, the observed TCDD-mediated decrease in ATP production was prevented by cotreatment with either AHR antagonist, indicating a role of the AHR in this effect of TCDD (Fig. 3D).

Besides altering the expression of key components of the ETC, TCDD decreased RNAs associated with oxidative stress defense mechanisms within the mitochondria (Fig. 3A), the primary source of reactive oxygen species (ROS) within the cell (Chance *et al.,* 1979; Chomyn and Attardi, 2003). In response to TCDD, mitochondrial GSR was decreased 3.1-fold by microarray (Fig. 3A, Supplementary table S4). This decrease was verified by qRT-PCR (Fig. 4A, left), and shown to be prevented by cotreatment with either AHR antagonist, ANF, or CH223191 (Supplemental fig. 2). Furthermore, mitochondrial GSR activity was measured, showing a 30% reduction in response to TCDD (Fig. 4A, right). GSR catalyzes the reduction of GSSG, thereby forming two molecules of reduced GSH. Based upon the observed decrease in mitochondrial GSR activity, we next measured mitochondrial GSH, in both the reduced and oxidized forms. Mitochondrial GSH was significantly decreased by 20% (Fig. 4B, left) whereas mitochondrial GSSG was significantly increased by 35% (Fig. 4B, right). This net effect to decrease the GSH/GSSG ratio is indicative of increased oxidative stress within the mitochondria. GSH is actively transported across mitochondrial membranes; however, GSSG cannot be transported out of the mitochondria (Olafsdottir and Reed, 1988). Therefore, GSSG remains in the mitochondria until it is reduced by GSR. Because of the lower mitochondrial GSR activity, we expected an increased oxidative state as a result of TCDD exposure. To test this prediction, we measured the mitochondrial production of the ROS, H_2O_2. TCDD increased mitochondrial ROS 151% (Fig. 4C), which was prevented by the addition of catalase, 500 U/ml (data not shown).

TCDD Impairs Glycolysis

Because some studies have linked glucose deprivation to mitochondrial stress (Ahmad *et al.,* 2005; Liu *et al.,* 2003), we investigated this connection as a possible mechanism by which TCDD mediates mitochondrial stress. Glucose enters NHEKs through glucose transporters encoded by Solute Carrier Family 2 (facilitated glucose transporter), members 1, 2, 3, and 5 (SLC2A1, 2, 3, and 5, formerly known as GLUT1, 2, 3, and 5). SLC2A1, 2, and 5 are known to be decreased during keratinocyte differentiation (Gherzi *et al.,* 1992; Shen *et al.,* 2000). Microarray analysis revealed that TCDD decreased the expression of SLC2A1, as well as the expression of six genes coding for glycolytic enzymes and lactate dehydrogenase A (Fig. 5A). Evaluation by qRT-PCR revealed that the levels of transcripts of genes encoding each step of the glycolysis pathway were significantly decreased in response to TCDD (Fig. 5B). Cotreatment studies using the AHR antagonists, ANF and CH223191, showed that the TCDD-mediated repression of 82% (9/11) of the glycolysis transcripts was abolished by cotreatment with an antagonist (Fig. 5B). Of interest, 78% (7/9) of these putative AHR-regulated transcripts showed significant increases in their levels of expression in the antagonist-treatment group (minus TCDD) relative to the control group (minus TCDD) (Fig. 5B), suggesting that the AHR may play a role in their constitutive regulation. By metabolomic analysis, we showed that the effect of TCDD to decrease SLC2A1 expression was accompanied by a decreased amount of intracellular glucose (Fig. 5C, top left). Additionally, by 48 h of

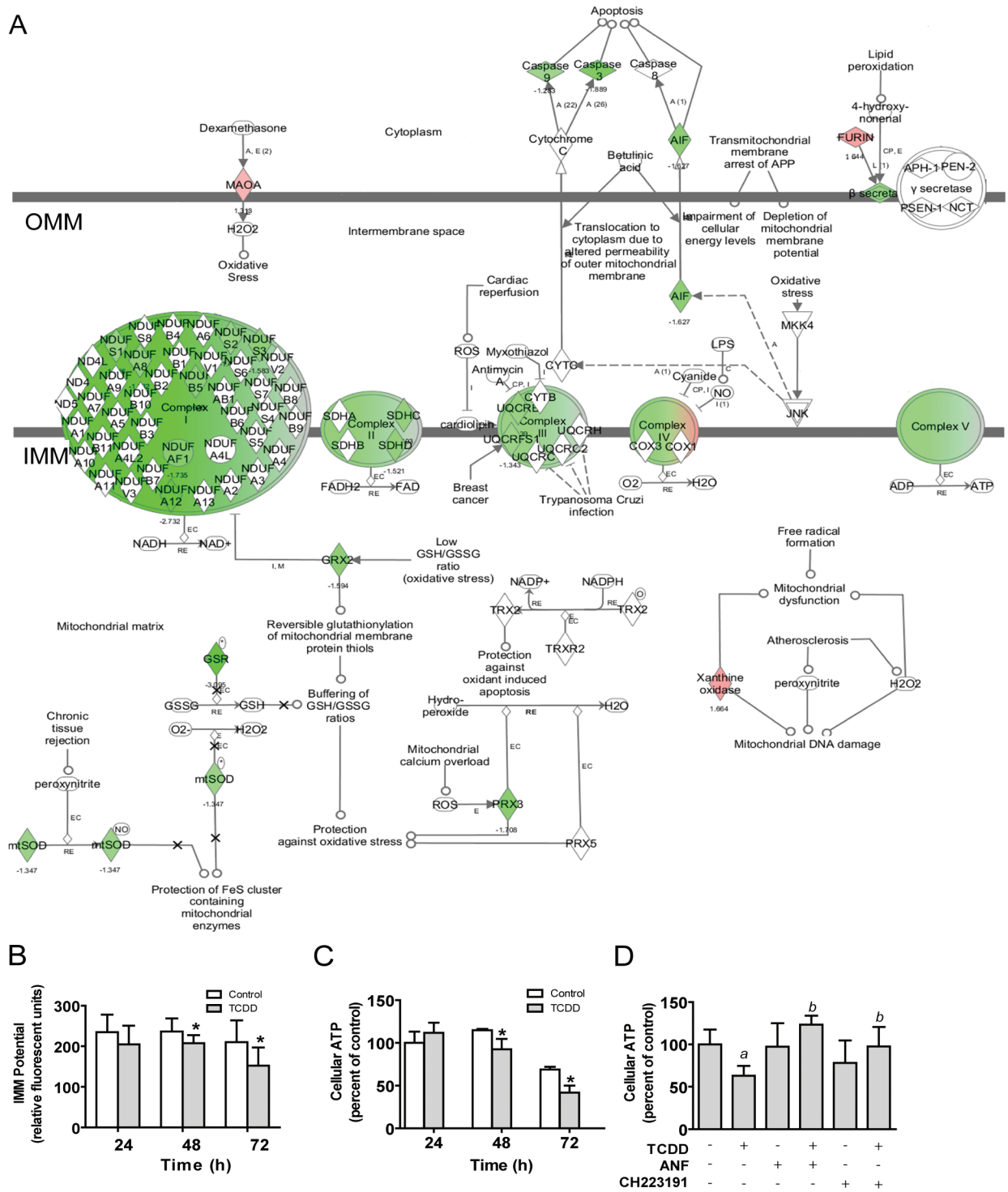

FIG. 3. TCDD impairs mitochondrial function. (A) Microarray analysis was performed using IPA. Depiction indicates TCDD-mediated (24 h) mitochondrial dysfunction in NHEKs. Green indicates decreased levels of RNA (treated/control); red indicates increased levels. Coloration of the ETC complexes indicates regulation of genes within the complex which may or may not be individually depicted. Individual genes are listed in Supplementary table S4. IMM, inner mitochondrial membrane; OMM, outer mitochondrial membrane. (B) and (C) NHEKs were treated for the indicated times. (B) IMM potential was measured as described in the Materials and Methods section (mean [$n = 8$] ± SD). (C) Levels of cellular ATP were measured using CL as described in the Materials and Methods section (mean [$n = 4$] ± SD), expressed as the percent of the 24 h control sample. *$p < 0.05$ indicates a significant difference between the time-matched control and treated samples. (D) NHEKs were treated with or without TCDD for 72 h in the presence or absence of the indicated AHR antagonists. Levels of cellular ATP were measured as in (C), above; *a* indicates a significant difference between the control and TCDD-treated samples; *b* indicates a significant difference between TCDD alone-treated samples and the TCDD plus AHR antagonist-treated samples, $p < 0.05$.

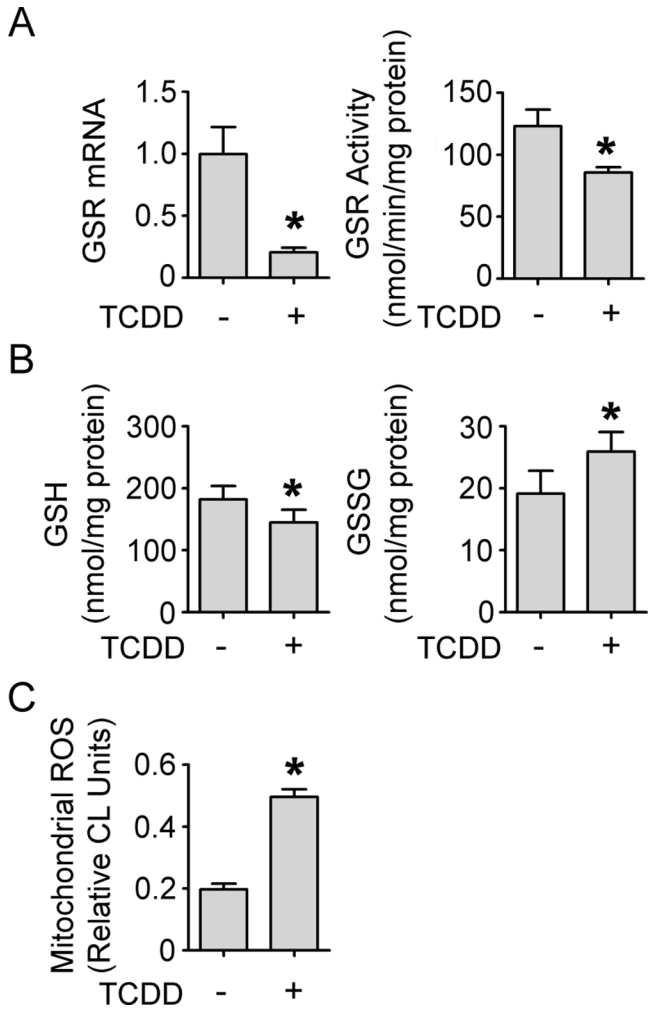

FIG. 4. TCDD increases mitochondrial oxidative stress. (A, left) qRT-PCR was used to verify TCDD-mediated (24 h) decreases observed in microarray analysis of mitochondrial GSR. Levels of RNA (mean [n = 4] ± SD) are expressed in units relative to the DMSO control, given a value of one. (A, right) Mitochondrial GSR activity was measured following TCDD treatment (24 h) as described in the Materials and Methods section (mean [n = 3] ± SD). (B) Levels of mitochondrial GSH (left) and GSSG (right) were measured following TCDD treatment (24 h) as described in the Materials and Methods section (mean [n = 3] ± SD). (C) Levels of mitochondrial H_2O_2 were measured following TCDD treatment (24 h) using CL as described in the Materials and Methods section (mean [n = 3] ± SD). *$p < 0.05$ indicates a significant difference between the control and treated samples.

treatment, TCDD significantly decreased the levels of nine glycolytic intermediates (Fig. 5C). This effect occurred ~24 h before the control cells showed similar decreases. Furthermore, lactate was also decreased, indicating that pyruvate was not being converted to lactate through fermentation. The next step in energy metabolism is the Krebs cycle, which links glycolysis to the ETC. Citrate is the first intermediate in the Krebs cycle. NADH is produced by the Krebs cycle and during glycolysis. Both NADH and succinate, also produced in the Krebs cycle, are used as reducing equivalents and are critical to the function of the ETC. Citrate, succinate, and NADH were significantly decreased by TCDD at 48 h, the same time when the glycolytic intermediates were decreased (Fig. 5D), indicating a possible loss of Krebs cycle efficiency. Furthermore, NAD^+ was significantly increased at 72 h (Fig. 5D), demonstrating that reducing equivalents were being consumed. Thus, we observed an overall decrease in energy metabolism and an increased cellular oxidative state.

Antioxidants Abrogate the Effect of TCDD to Accelerate Keratinocyte Differentiation

In cultures of NHEKs, inducers of mitochondrial dysfunction such as rotenone and staurosporine have been shown to increase early markers of keratinocyte differentiation, KRT10 and involucrin, and conversely, antioxidants have been shown to block this induction of KRT10 (Tamiji *et al.,* 2005). It has also been suggested that accumulation of ROS, inducing mitochondrial impairment, may be a prerequisite for keratinocyte differentiation (Hornig-Do *et al.,* 2007). To test the hypothesis that TCDD-induced acceleration of NHEK differentiation is mediated by increased levels of ROS, we measured the percentage CE formation in cultures of NHEKs treated with TCDD in the presence or absence of two chemical antioxidants, DPPD and quercetin, and the enzyme catalase which catalyzes the decomposition of H_2O_2 to water and oxygen. All three antioxidants blocked the TCDD-induced increase in CE formation (Fig. 6A), indicating an important role of H_2O_2 production in the mechanism of action of TCDD to accelerate terminal differentiation. However, because both chemical antioxidants, due to their chemical structure, may interact with the AHR and thereby compete with TCDD for AHR binding, we extended these studies to include the widely used antioxidant, NAC, which also blocked the TCDD-induced increase in CE formation (Fig. 6B). Furthermore, although extracellular catalase has been reported and shown here to decrease levels of intracellular ROS (Jing *et al.,* 2012; Supplementary fig. S3), we extended these studies to include PEG-catalase, reported to have improved cellular uptake (Beckman *et al.,* 1988). Both extracellular catalase and PEG-catalase blocked the effect of TCDD to enhance keratinocyte differentiation (Fig. 6B). This effect of TCDD to accelerate terminal differentiation was also blocked by the cotreatment with the AHR antagonist CH223191, indicating that this response to TCDD is mediated by the AHR (Fig. 6B).

DISCUSSION

In humans exposed to dioxin, chloracne is considered the "hallmark" toxicity of this exposure, as it is the most visible and commonly observed response (Panteleyev and Bickers, 2006; Suskind, 1985) Here, using NHEKs as a model of the actions of TCDD to affect the interfollicular squamous epithelium, we showed that the major gene ontology category enriched by genes having increased levels of RNA expression

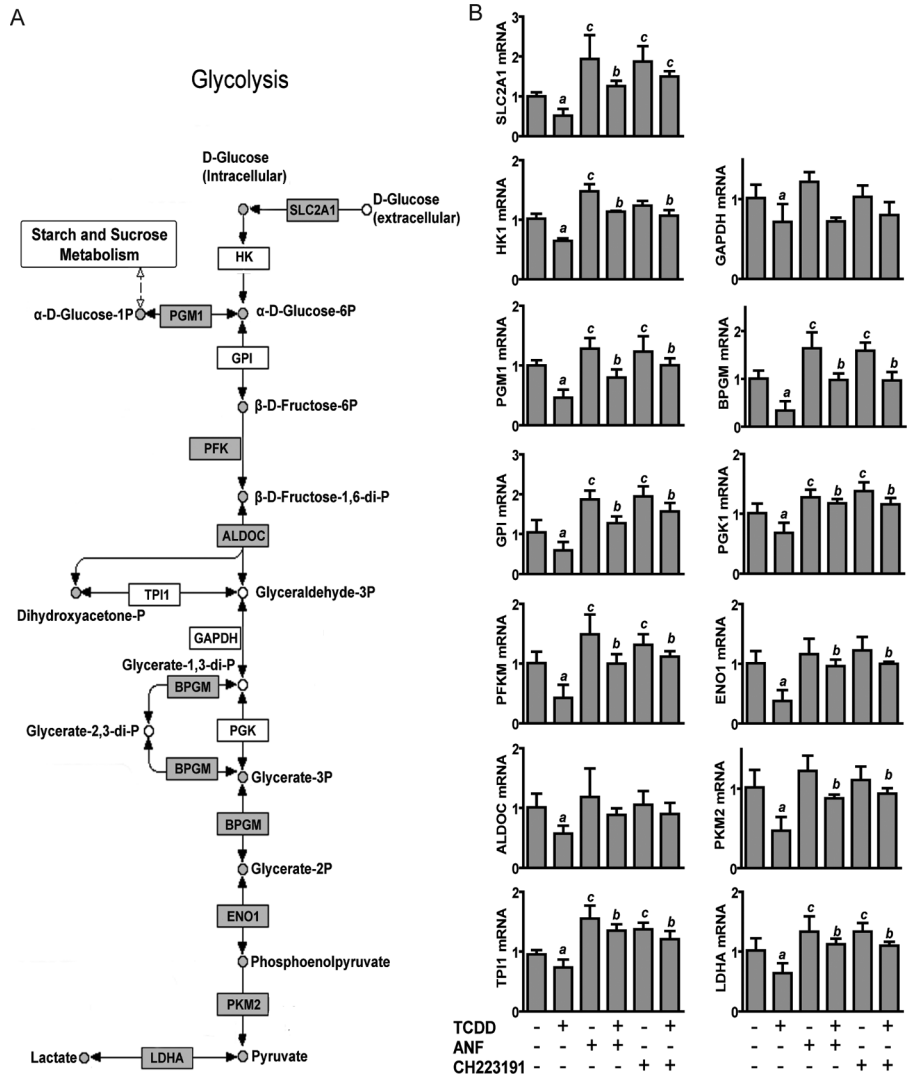

FIG. 5. TCDD decreases glycolysis. (A) The glycolytic pathway adapted from the KEGG pathway database. Gray boxes indicate decreased RNA expression by TCDD (24 h) based on microarray analysis (Supplementary table S4); white boxes were not significant. Gray circles indicate the biochemical products that were decreased by TCDD, based on the metabolomic data presented in (C). White circles indicate the biochemical products that were not measured. (B) Validation of transcript levels for SLC2A1 and the glycolysis pathway. NHEKs were treated with or without TCDD for 24 h in the presence or absence of the indicated AHR antagonists. Levels of RNA were measured by qRT-PCR. *a* indicates a significant difference between the control and TCDD-treated samples; *b* indicates a significant difference between TCDD alone- and the TCDD plus AHR antagonist–treated samples; *c* indicates a significant difference between control and AHR antagonist–treated samples, $p < 0.05$. Note that HK1, GPI, TPI1, GAPDH, and PGK1 were decreased significantly in response to TCDD as measured by qRT-PCR analysis, in comparison to the microarray analysis. (C) Quantitation by LC/GC-MS of the glycolytic pathway intermediates following treatment for the indicated times with control or TCDD. (D) Quantitation by LC/GC-MS of citrate, succinate, NADH, and NAD^+, following treatment for the indicated times with control or TCDD. $*p < 0.05$ indicates a significant difference between the time-matched control and treated samples ($n = 5$). ND indicates that the compound was not detected in at least three of the five samples in a group.

in response to TCDD was the biological process termed *epidermal differentiation*. Among the genes in this category were 40% of the genes of the EDC, a 1.6 Mbp region of chromosome 1q21 encoding genes that produce the cornified envelope. These results confirm and expand on our earlier publications of this effect of TCDD (Sutter *et al.,* 2011). Moreover, we identified 203 additional genes that are known to participate in epidermal differentiation. The major functional categories represented by these genes include structural protein of the cornified envelope, lipid metabolism, antimicrobial activity, protease, protease inhibitor and extracellular matrix protein, cell-cell interaction, transporter, transcription factor, and signaling. In general, the expression levels of most of the genes were increased from two- to fourfold. Together, the identification of these genes provides a greatly improved understanding of the effects of TCDD to accelerate keratinocyte differentiation. Although these results are consistent with the accepted idea that the persistent action of TCDD to enhance epidermal differentiation ultimately

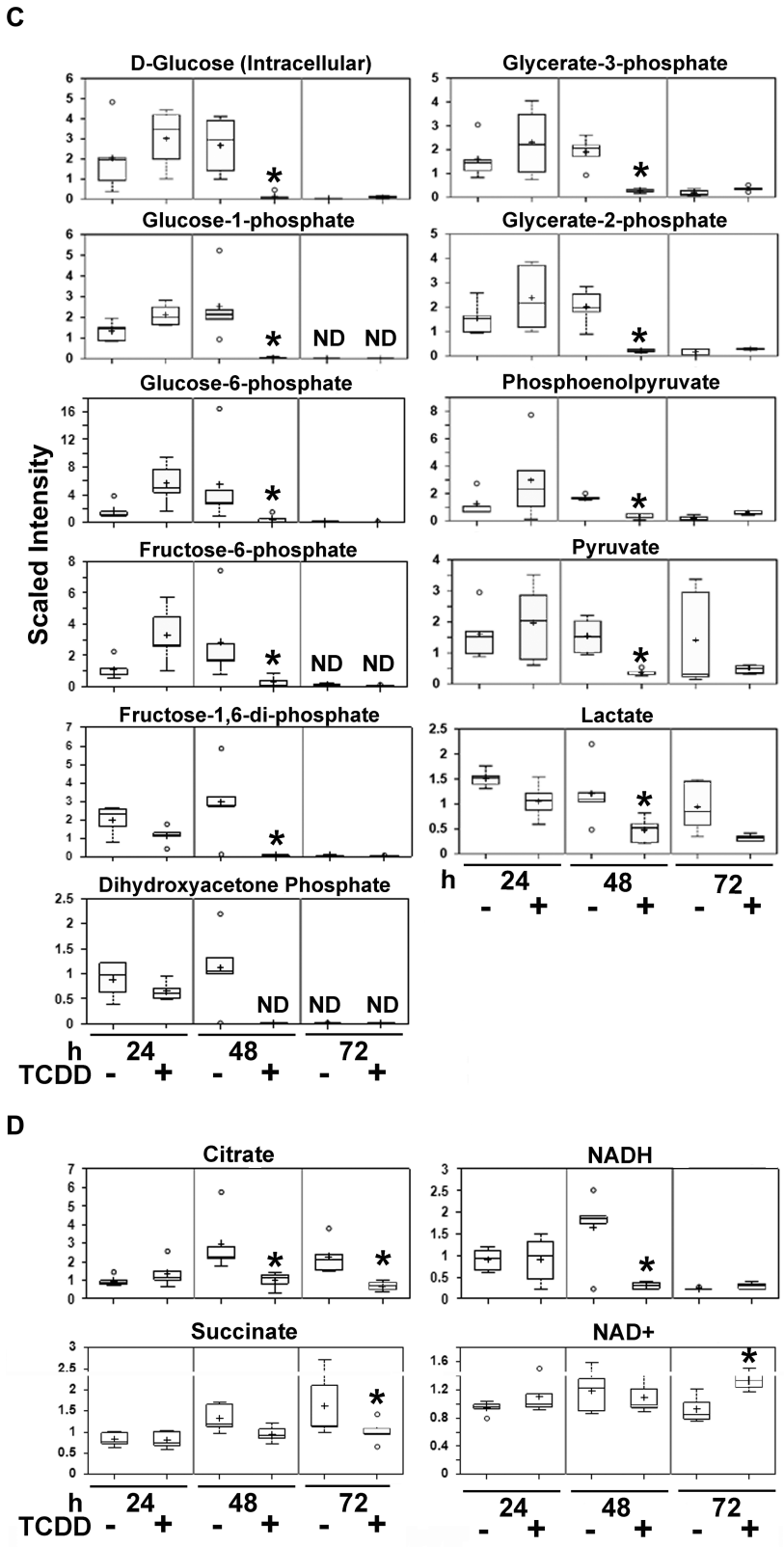

FIG. 5. Continued

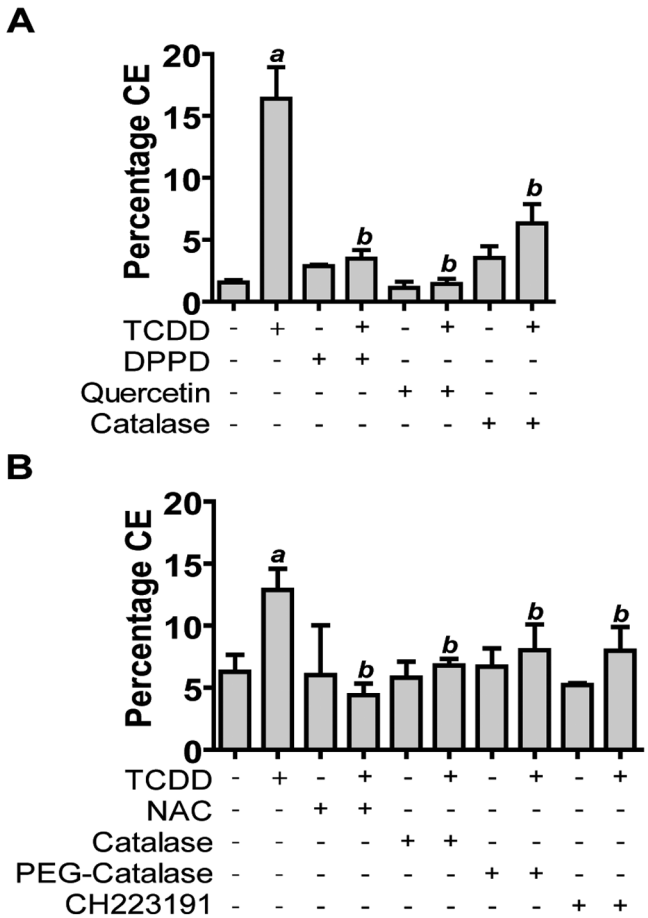

FIG. 6. Antioxidants block the effect of TCDD to increase keratinocyte differentiation. (A) CEs were isolated after treatment, control or TCDD for 72 h in the presence or absence of one of the following antioxidants: DPPD (2.5μM), quercetin (10μM), or catalase (500 U/ml). *a* indicates a significant difference between the control and TCDD-treated samples (mean [$n = 4$] ± SD); *b* indicates a significant difference between TCDD alone- and the TCDD plus antioxidant–treated samples, $p < 0.05$. (B) CEs were isolated after treatment, control, or TCDD for 72 h in the presence or absence of one of the antioxidants, NAC (1.25mM), catalase (500 U/ml), PEG-catalase (1000 U/ml), or the AHR antagonist, CH223191 (1μM). *a* indicates a significant difference between the control and TCDD-treated samples (mean [$n = 4$] ± SD); *b* indicates a significant difference between TCDD alone- and the TCDD plus antioxidant- or antagonist-treated samples, $p < 0.05$.

disrupts skin homeostasis (Sutter *et al.,* 1991), insights into two additional mechanisms of TCDD toxicity are evident in these data, namely, imbalanced stoichiometry of the constituents of the cornified envelope and the recruitment of novel transcripts into pathways essential for differentiation.

In the epidermis, loricrin is a major protein comprising more than 80% of the total protein of the cornified envelope. The SPRR proteins comprise a much smaller percentage, and the ratio of SPRRs to loricrin is known to vary from < 1:100 in the thinner trunk epidermis to ~1:10 in thicker palmo-plantar epidermis. Crosslinking of SPRRs to loricrin by transglutaminase 3 acts to solubilize the relatively insoluble loricrin protein, and the specific SPRR content is believed to promote the biomechanical properties of flexibility or rigidity and toughness of the epidermis, as required for its function in localized regions of the body (Candi *et al.,* 2005). In addition to providing a mechanism to control the expression and concentration of these CE structural proteins in manner that supports tissue specific biomechanical requirements, the organization of these multigene families of the EDC also allows for specific adaptive responses to environmental insults (Cabral *et al.,* 2001b). TCDD appears to act as such an insult. For example, the expression of SPRR4 was increased about fourfold in response to TCDD. SPRR4 is normally expressed at very low or undetectable levels both *in vitro* and *in vivo* (Cabral *et al.,* 2001a). However, SPRR4 is induced by chronic UV exposure and is associated with fragile cornified envelopes and epidermal hyperplasia (Cabral *et al.,* 2001a). Similarly, the expression of LCE3A was increased about 12-fold in response to TCDD. Although LCE3A is expressed at very low levels in normal human skin (Jackson *et al.,* 2005), its expression is markedly increased in response to disruption of the epidermal barrier by tape stripping (Bergboer *et al.,* 2011). Thus, similar to the response to other environmental insults, the relative changes in the ratios of expression of the genes whose products make up the cornified envelope may alter the function of the epidermis upon exposure to TCDD.

Analogous to the structure of the corneocyte, specific ratios of the neutral lipids, which comprise the lipid matrix, cholesterol, FFA, and Cer, must exist in order for the epidermal permeability barrier to properly function (Man *et al.,* 1993). Moreover, an increase in the ratio of Cer to FFA has been found in patients with lamellar ichthyosis (Lavrijsen *et al.,* 1995), and increased levels of Cer 7 have been associated with atopic dermatitis (Jungersted *et al.,* 2010). Here, we showed that TCDD increased Cer; this effect paralleled the increase of the *de novo* Cer synthesis pathway, as well as the expression of UGCG, which produces GCer, and GBA, responsible for the production of Cer 1, 4, 9 and Cer 3, 6, 7, from acyl-GCer and GCer, respectively (Uchida and Holleran, 2008). Although the amounts of each Cer, with the exception of Cer 8, were significantly increased, neither cholesterol nor FFA content changed. The consequence of this effect is an increased ratio of Cer to FFA in the TCDD-treated samples, which would likely lead to impaired barrier function of the epidermis, as seen in lamellar ichthyosis.

For the genes whose expression levels were decreased in response to TCDD, the most significantly enriched gene ontology category was the cellular component, *mitochondrion*. The effects of TCDD to increase oxidative stress (Stohs, 1990) and impair mitochondrial function have been reported in studies of multiple species, tissues, and cells (Aly and Domenech, 2009; Biswas *et al.,* 2008; Chen *et al.,* 2010; Fisher *et al.,* 2005; Latchoumycandane *et al.,* 2002; Senft *et al.,* 2002a,b; Shen *et al.,* 2005; Shertzer *et al.,* 2006). Although the effect to increase ROS is common to these studies, other functional endpoints have been inconsistently measured, and in some cases, with contrary results. ATP production was reported to decrease

in TCDD-treated keratinocytes (this study), human trophoblast-like JAR cells (Chen *et al.,* 2010) and C57BL/6J mouse liver (Senft *et al.,* 2002b; Shertzer *et al.,* 2006). Although IMM potential was reported to decrease in TCDD-exposed keratinocytes (this study), human JAR cells (Chen *et al.,* 2010), C2C12 rhabdomyoblasts (61), rat hepatocytes (Aly and Domenech, 2009), and C57BL/6 epididydimal spermatozoa (Fisher *et al.,* 2005), mitochondrial membrane hyperpolarization was reported in the livers of C57BL/6J mice (Shen *et al.,* 2005). In addition, livers of C57BL/6J mice also showed an increase in GSR activity (Senft *et al.,* 2002a), as well as an increased mitochondrial GSH/GSSG ratio (Shen *et al.,* 2005), leading these authors to propose that TCDD increases the production of mitochondrial ROS as the result of an overall increase in the reductive state of the mitochondria (Senft *et al.,* 2002b; Shen *et al.,* 2005; Shertzer *et al.,* 2006). Here in keratinocytes, the increase in mitochondrial ROS production is consistent with an oxidative state of the mitochondria as mitochondrial GSR activity is decreased, as is the GSH/GSSG ratio. Similar TCDD-mediated reductions in GSR activity have been reported in studies of the effects of TCDD on rat testis, *in vivo* (Latchoumycandane *et al.,* 2002), and cultures of isolated rat hepatocytes (Aly and Domenech, 2009). The effects of TCDD on NHEKs to decrease the expression of mitochondrial GSR and superoxide dismutase and to increase the expression of xanthine oxidase and monoamine oxidase A are likely to contribute to the increased oxidative state of the mitochondria. However, it is important to note that the TCDD-mediated induction of cytochrome P450 is another important source of intracellular ROS (Kopf and Walker, 2010; Park *et al.,* 1996), and given the 96- and 69-fold TCDD-mediated increases in the expression of CYP1A1 and CYP1B1, respectively, observed in this study (data not shown), the contribution of this pathway warrants further study. TCDD also alters the expression of many additional nuclear-encoded mitochondrial genes, and similar effects have been recently reported in both mice and rats (Forgacs *et al.,* 2010; Forman *et al.,* 2010). Together, these effects on gene expression likely contribute to the observed changes in IMM potential, increased ROS, and decreased ATP production. Furthermore, by LC/GC-MS, we determined that the levels of pyruvate, citrate, succinate, and NADH were decreased by 48 h of treatment. This was followed by an increase in the level of NAD^+ at 72 h. This overall reduction in reducing equivalents should also contribute to the decreased functioning of the mitochondria and the observed increase in mitochondrial ROS production. In fact, pyruvate has been shown to act as an antioxidant, reacting with H_2O_2 and organic hydroperoxides (Nath *et al.,* 1995).

In some cells such as rat hepatocytes, TCDD-mediated increases in ROS have been associated with cytotoxicity (Aly and Domenech, 2009). In mouse liver, TCDD-mediated increases in ROS have been associated with increased levels of oxidative DNA adducts (Shen *et al.,* 2005), and this effect has been suggested to contribute to the carcinogenic effects of TCDD. However, in other cells types such as the human trophoblast–like JAR cells, TCDD-mediated ROS results in apoptosis (Chen *et al.,* 2010). In addition to its harmful effects, ROS are also understood to function as regulators of signaling pathways (Finkel, 2011; Forman *et al.,* 2010), contributing to the regulation of cellular processes that include growth factor stimulation, inflammation, apoptosis, and cell proliferation and differentiation (Finkel, 2011; Forman *et al.,* 2010). Among ROS, H_2O_2 has been proposed to have the chemical properties that best fulfill the requirements of a second messenger, i.e., its enzymatic production and degradation provide the necessary specificity for controlling its half-life and location, and its chemistry provides for its specificity for oxidation of thiols (Forman *et al.,* 2010). The mechanisms of keratinocyte differentiation that lead to the formation of the corneocyte are not well understood. They involve the crosslinking of numerous proteins, degradation of organelles, and the fusion of lamellar bodies into the plasma membrane. Ultimately, these cells undergo a specialized form of programmed cell death, with characteristics that distinguish it from either apoptosis or autophagy (Lippens *et al.,* 2000; Mitra *et al.,* 1997). Although differentiating keratinocytes have certain events in common with apoptosis such as decreases in IMM potential and increases in ROS and cytochrome *c* release, these events are believed to regulate a unique process designed to produce and maintain the epidermal barrier (Grether-Beck *et al.,* 2003). Here, we demonstrated that TCDD affected CE formation by increasing cellular ROS. When TCDD-enhanced ROS was decreased by the addition of chemical antioxidants or antioxidant enzymes, TCDD-mediated corneocyte formation was inhibited. Moreover, studies with the AHR antagonist CH223191 indicated that this TCDD-mediated cell differentiation was AHR dependent. Together, these results provide compelling evidence supporting the role of TCDD-mediated production of ROS as an essential step in the mechanism of action to accelerate keratinocyte differentiation. These results support a possible signaling role for H_2O_2 that is further supported by our previously published results showing that TCDD is not toxic to the keratinocytes under the concentrations and times of treatment used in this study (Sutter *et al.,* 2010). However, the redox state of cell, including the ratio of NAD^+/NADH, plays a central role in the integration of energy metabolism and cellular signaling (Koch-Nolte *et al.,* 2011). This understanding coupled with the recent report of the role of TCDD-inducible poly(ADP-ribose) polymerase in the suppression of hepatic gluconeogenesis (Diani-Moore *et al.,* 2010) indicates the likely complexity of the mechanism underlying the biochemical responses to TCDD reported here.

A unique finding of this study was that TCDD decreased glycolysis. Mitochondria require reducing equivalents to produce ATP; these equivalents are NADH and succinate. NADH is produced during glycolysis and both NADH and succinate are produced by the Krebs cycle, which obtains its initiating substrate, acetyl-CoA, from glycolysis via the pyruvate dehydrogenase complex, which converts pyruvate to acetyl-CoA. Thus, a downregulation of glycolysis would ultimately lead

to lower concentrations of reducing equivalents and decreased mitochondrial function, as observed.

TCDD has been reported to downregulate the expression of several glucose transporters, including SLC2A4, in 3T3-L1 adipocytes (Liu and Matsumura, 2006) and SLC2A1 and 3 in the embryonic carcinoma cell line P19 (Tonack *et al.,* 2007). In the latter study, this effect of TCDD was shown to be mediated by the AHR and to result in lower glucose uptake in the P19 embryoid bodies (Tonack *et al.,* 2007). In the epidermis, keratinocyte differentiation is associated with decreased expression of SLC2A1, 2, and 5 (Gherzi *et al.,* 1992; Shen *et al.,* 2000). In other cell lines, glucose deprivation has been associated with impaired mitochondrial function and oxidative stress (Ahmad *et al.,* 2005; Liu *et al.,* 2003). Together, these published observations and the results presented here suggest a possible mechanism whereby TCDD-mediated repression of SLC2A1 and key glycolytic enzymes leads to impaired mitochondrial function and increased production of H_2O_2, and/or an increased ratio of NAD^+/NADH, which act as second messengers to enhance terminal differentiation of NHEKs.

SUPPLEMENTARY DATA

Supplementary data are available online at http://toxsci.oxfordjournals.org/.

FUNDING

National Institutes of Health (R01 ES017014); W. Harry Feinstone Center for Genomic Research; Department of the Navy Permanent Military Professor Program.

ACKNOWLEDGMENTS

We thank Dr Shirlean Goodwin for assistance with the microarray assay, Gayatri Mamidanna for assistance with the CE assays, Ryan Wible for helpful discussions of chromatographic theory, and the Integrated Microscopy Center at the University of Memphis for use of the confocal microscope.

REFERENCES

Abramoff, M. D., Magalhaes, P. J., and Ram, S. J. (2004). Image processing with ImageJ. *Biophoton. Int.* **11,** 36–42.

Ahmad, I. M., Aykin-Burns, N., Sim, J. E., Walsh, S. A., Higashikubo, R., Buettner, G. R., Venkataraman, S., Mackey, M. A., Flanagan, S. W., Oberley, L. W., *et al.* (2005). Mitochondrial O_2*- and H_2O_2 mediate glucose deprivation-induced stress in human cancer cells. *J. Biol. Chem.* **280,** 4254–4263.

Aly, H. A., and Domenech, O. (2009). Cytotoxicity and mitochondrial dysfunction of 2,3,7,8-tetrachlorodibenzo-p-dioxin (TCDD) in isolated rat hepatocytes. *Toxicol. Lett.* **191,** 79–87.

Beckman, J. S., Minor, R. L. Jr., White, C. W., Repine, J. E., Rosen, G. M., and Freeman, B. A. (1988). Superoxide dismutase and catalase conjugated to polyethylene glycol increases endothelial enzyme activity and oxidant resistance. *J. Biol. Chem.* **263,** 6884–6892.

Benjamini, Y., and Hochberg, Y. (1995). Controlling the false discovery rate: A practical and powerful approach to multiple testing. *J. R. Stat. Soc.* **57,** 11.

Bergboer, J. G., Tjabringa, G. S., Kamsteeg, M., van Vlijmen-Willems, I. M., Rodijk-Olthuis, D., Jansen, P. A., Thuret, J. Y., Narita, M., Ishida-Yamamoto, A., Zeeuwen, P. L., *et al.* (2011). Psoriasis risk genes of the late cornified envelope-3 group are distinctly expressed compared with genes of other LCE groups. *Am. J. Pathol.* **178,** 1470–1477.

Biswas, G., Srinivasan, S., Anandatheerthavarada, H. K., and Avadhani, N. G. (2008). Dioxin-mediated tumor progression through activation of mitochondria-to-nucleus stress signaling. *Proc. Natl. Acad. Sci. U.S.A.* **105,** 186–191.

Breiden, B., Gallala, H., Doering, T., and Sandhoff, K. (2007). Optimization of submerged keratinocyte cultures for the synthesis of barrier ceramides. *Eur. J. Cell Biol.* **86,** 657–673.

Cabral, A., Sayin, A., de Winter, S., Fischer, D. F., Pavel, S., and Backendorf, C. (2001a). SPRR4, a novel cornified envelope precursor: UV-dependent epidermal expression and selective incorporation into fragile envelopes. *J. Cell. Sci.* **114**(Pt 21), 3837–3843.

Cabral, A., Voskamp, P., Cleton-Jansen, A. M., South, A., Nizetic, D., and Backendorf, C. (2001b). Structural organization and regulation of the small proline-rich family of cornified envelope precursors suggest a role in adaptive barrier function. *J. Biol. Chem.* **276,** 19231–19237.

Candi, E., Schmidt, R., and Melino, G. (2005). The cornified envelope: A model of cell death in the skin. *Nat. Rev. Mol. Cell Biol.* **6,** 328–340.

Chance, B., Sies, H., and Boveris, A. (1979). Hydroperoxide metabolism in mammalian organs. *Physiol. Rev.* **59,** 527–605.

Chen, S. C., Liao, T. L., Wei, Y. H., Tzeng, C. R., and Kao, S. H. (2010). Endocrine disruptor, dioxin (TCDD)-induced mitochondrial dysfunction and apoptosis in human trophoblast-like JAR cells. *Mol. Hum. Reprod.* **16,** 361–372.

Chomyn, A., and Attardi, G. (2003). MtDNA mutations in aging and apoptosis. *Biochem. Biophys. Res. Commun.* **304,** 519–529.

Crompton, M. (1999). The mitochondrial permeability transition pore and its role in cell death. *Biochem. J.* **341,** 233–249.

Dehaven, C. D., Evans, A. M., Dai, H., and Lawton, K. A. (2010). Organization of GC/MS and LC/MS metabolomics data into chemical libraries. *J. Cheminform.* **2,** 9.

Diani-Moore, S., Ram, P., Li, X., Mondal, P., Youn, D. Y., Sauve, A. A., and Rifkind, A. B. (2010). Identification of the aryl hydrocarbon receptor target gene TiPARP as a mediator of suppression of hepatic gluconeogenesis by 2,3,7,8-tetrachlorodibenzo-p-dioxin and of nicotinamide as a corrective agent for this effect. *J. Biol. Chem.* **285,** 38801–38810.

Evans, A. M., DeHaven, C. D., Barrett, T., Mitchell, M., and Milgram, E. (2009). Integrated, nontargeted ultrahigh performance liquid chromatography/electrospray ionization tandem mass spectrometry platform for the identification and relative quantification of the small-molecule complement of biological systems. *Anal. Chem.* **81,** 6656–6667.

Finkel, T. (2011). Signal transduction by reactive oxygen species. *J. Cell Biol.* **194,** 7–15.

Fisher, M. T., Nagarkatti, M., and Nagarkatti, P. S. (2005). Aryl hydrocarbon receptor-dependent induction of loss of mitochondrial membrane potential in epididydimal spermatozoa by 2,3,7,8-tetrachlorodibenzo-p-dioxin (TCDD). *Toxicol. Lett.* **157,** 99–107.

Forgacs, A. L., Burgoon, L. D., Lynn, S. G., LaPres, J. J., and Zacharewski, T. (2010). Effects of TCDD on the expression of nuclear encoded mitochondrial genes. *Toxicol. Appl. Pharmacol.* **246,** 58–65.

Forman, H. J., Maiorino, M., and Ursini, F. (2010). Signaling functions of reactive oxygen species. *Biochemistry* **49,** 835–842.

Gherzi, R., Melioli, G., de Luca, M., D'Agostino, A., Distefano, G., Guastella, M., D'Anna, F., Franzi, A. T., and Cancedda, R. (1992). "HepG2/erythroid/

brain" type glucose transporter (GLUT1) is highly expressed in human epidermis: Keratinocyte differentiation affects GLUT1 levels in reconstituted epidermis. *J. Cell. Physiol.* **150,** 463–474.

Gray, G. M., and Yardley, H. J. (1975). Different populations of pig epidermal cells: Isolation and lipid composition. *J. Lipid Res.* **16,** 441–447.

Greenlee, W. F., Dold, K. M., and Osborne, R. (1985). Actions of 2,3,7,8-tetrachlorodibenzo-p-dioxin (TCDD) on human epidermal keratinocytes in culture. *In Vitro Cell. Dev. Biol.* **21,** 509–512.

Grether-Beck, S., Felsner, I., Brenden, H., and Krutmann, J. (2003). Mitochondrial cytochrome c release mediates ceramide-induced activator protein 2 activation and gene expression in keratinocytes. *J. Biol. Chem.* **278,** 47498–47507.

Hamanaka, S., Hara, M., Nishio, H., Otsuka, F., Suzuki, A., and Uchida, Y. (2002). Human epidermal glucosylceramides are major precursors of stratum corneum ceramides. *J. Invest. Dermatol.* **119,** 416–423.

Homayouni, R., Heinrich, K., Wei, L., and Berry, M. W. (2005). Gene clustering by latent semantic indexing of MEDLINE abstracts. *Bioinformatics* **21,** 104–115.

Hornig-Do, H. T., von Kleist-Retzow, J. C., Lanz, K., Wickenhauser, C., Kudin, A. P., Kunz, W. S., Wiesner, R. J., and Schauen, M. (2007). Human epidermal keratinocytes accumulate superoxide due to low activity of Mn-SOD, leading to mitochondrial functional impairment. *J. Invest. Dermatol.* **127,** 1084–1093.

Jackson, B., Tilli, C. M., Hardman, M. J., Avilion, A. A., MacLeod, M. C., Ashcroft, G. S., and Byrne, C. (2005). Late cornified envelope family in differentiating epithelia–response to calcium and ultraviolet irradiation. *J. Invest. Dermatol.* **124,** 1062–1070.

Jing, Y., Liu, L. Z., Jiang, Y., Zhu, Y., Guo, N. L., Barnett, J., Rojanasakul, Y., Agani, F., and Jiang, B. H. (2012). Cadmium increases HIF-1 and VEGF expression through ROS, ERK, and AKT signaling pathways and induces malignant transformation of human bronchial epithelial cells. *Toxicol. Sci.* **125,** 10–19.

Jungersted, J. M., Scheer, H., Mempel, M., Baurecht, H., Cifuentes, L., Høgh, J. K., Hellgren, L. I., Jemec, G. B., Agner, T., and Weidinger, S. (2010). Stratum corneum lipids, skin barrier function and filaggrin mutations in patients with atopic eczema. *Allergy* **65,** 911–918.

Koch-Nolte, F., Fischer, S., Haag, F., and Ziegler, M. (2011). Compartmentation of NAD+-dependent signalling. *FEBS Lett.* **585,** 1651–1656.

Kopf, P. G., and Walker, M. K. (2010). 2,3,7,8-Tetrachlorodibenzo-p-dioxin increases reactive oxygen species production in human endothelial cells via induction of cytochrome P4501A1. *Toxicol. Appl. Pharmacol.* **245,** 91–99.

Lampe, M. A., Williams, M. L., and Elias, P. M. (1983). Human epidermal lipids: Characterization and modulations during differentiation. *J. Lipid Res.* **24,** 131–140.

Latchoumycandane, C., Chitra, K. C., and Mathur, P. P. (2002). The effect of 2,3,7,8-tetrachlorodibenzo-p-dioxin on the antioxidant system in mitochondrial and microsomal fractions of rat testis. *Toxicology* **171,** 127–135.

Lavrijsen, A. P., Bouwstra, J. A., Gooris, G. S., Weerheim, A., Boddé, H. E., and Ponec, M. (1995). Reduced skin barrier function parallels abnormal stratum corneum lipid organization in patients with lamellar ichthyosis. *J. Invest. Dermatol.* **105,** 619–624.

Lippens, S., Kockx, M., Knaapen, M., Mortier, L., Polakowska, R., Verheyen, A., Garmyn, M., Zwijsen, A., Formstecher, P., Huylebroeck, D., *et al.* (2000). Epidermal differentiation does not involve the pro-apoptotic executioner caspases, but is associated with caspase-14 induction and processing. *Cell Death Differ.* **7,** 1218–1224.

List, K., Currie, B., Scharschmidt, T. C., Szabo, R., Shireman, J., Molinolo, A., Cravatt, B. F., Segre, J., and Bugge, T. H. (2007). Autosomal ichthyosis with hypotrichosis syndrome displays low matriptase proteolytic activity and is phenocopied in ST14 hypomorphic mice. *J. Biol. Chem.* **282,** 36714–36723.

Liu, P. C., and Matsumura, F. (2006). TCDD suppresses insulin-responsive glucose transporter (GLUT-4) gene expression through C/EBP nuclear transcription factors in 3T3-L1 adipocytes. *J. Biochem. Mol. Toxicol.* **20,** 79–87.

Liu, Y., Song, X. D., Liu, W., Zhang, T. Y., and Zuo, J. (2003). Glucose deprivation induces mitochondrial dysfunction and oxidative stress in PC12 cell line. *J. Cell. Mol. Med.* **7,** 49–56.

Loertscher, J. A., Sattler, C. A., and Allen-Hoffmann, B. L. (2001). 2,3,7,8-Tetrachlorodibenzo-p-dioxin alters the differentiation pattern of human keratinocytes in organotypic culture. *Toxicol. Appl. Pharmacol.* **175,** 121–129.

Man, M. Q., Feingold, K. R., and Elias, P. M. (1993). Exogenous lipids influence permeability barrier recovery in acetone-treated murine skin. *Arch. Dermatol.* **129,** 728–738.

Michibata, H., Chiba, H., Wakimoto, K., Seishima, M., Kawasaki, S., Okubo, K., Mitsui, H., Torii, H., and Imai, Y. (2004). Identification and characterization of a novel component of the cornified envelope, cornifelin. *Biochem. Biophys. Res. Commun.* **318,** 803–813.

Mitra, R. S., Wrone-Smith, T., Simonian, P., Foreman, K. E., Nunez, G., and Nickoloff, B. J. (1997). Apoptosis in keratinocytes is not dependent on induction of differentiation. *Lab. Invest.* **76,** 99–107.

Nath, K. A., Ngo, E. O., Hebbel, R. P., Croatt, A. J., Zhou, B., and Nutter, L. M. (1995). alpha-Ketoacids scavenge H_2O_2 in vitro and in vivo and reduce menadione-induced DNA injury and cytotoxicity. *Am. J. Physiol.* **268**(1), C227–C236.

Olafsdottir, K., and Reed, D. J. (1988). Retention of oxidized glutathione by isolated rat liver mitochondria during hydroperoxide treatment. *Biochim. Biophys. Acta* **964,** 377–382.

Panteleyev, A. A., and Bickers, D. R. (2006). Dioxin-induced chloracne–reconstructing the cellular and molecular mechanisms of a classic environmental disease. *Exp. Dermatol.* **15,** 705–730.

Paragh, G., Ugocsai, P., Vogt, T., Schling, P., Kel, A. E., Tarabin, V., Liebisch, G., Orsó, E., Markó, L., Balogh, A., *et al.* (2010). Whole genome transcriptional profiling identifies novel differentiation regulated genes in keratinocytes. *Exp. Dermatol.* **19,** 297–301.

Park, J. Y., Shigenaga, M. K., and Ames, B. N. (1996). Induction of cytochrome P4501A1 by 2,3,7,8-tetrachlorodibenzo-p-dioxin or indolo(3,2-b)carbazole is associated with oxidative DNA damage. *Proc. Natl. Acad. Sci. U.S.A.* **93,** 2322–2327.

Perry, D. K., Carton, J., Shah, A. K., Meredith, F., Uhlinger, D. J., and Hannun, Y. A. (2000). Serine palmitoyltransferase regulates de novo ceramide generation during etoposide-induced apoptosis. *J. Biol. Chem.* **275,** 9078–9084.

Pfaffl, M. W. (2001). A new mathematical model for relative quantification in real-time RT-PCR. *Nucleic Acids Res.* **29,** e45.

Ponec, M., and Weerheim, A. (1990). Retinoids and lipid changes in keratinocytes. *Meth. Enzymol.* **190,** 30–41.

Senft, A. P., Dalton, T. P., Nebert, D. W., Genter, M. B., Hutchinson, R. J., and Shertzer, H. G. (2002a). Dioxin increases reactive oxygen production in mouse liver mitochondria. *Toxicol. Appl. Pharmacol.* **178,** 15–21.

Senft, A. P., Dalton, T. P., Nebert, D. W., Genter, M. B., Puga, A., Hutchinson, R. J., Kerzee, J. K., Uno, S., and Shertzer, H. G. (2002b). Mitochondrial reactive oxygen production is dependent on the aromatic hydrocarbon receptor. *Free Radic. Biol. Med.* **33,** 1268–1278.

Senft, A. P., Dalton, T. P., and Shertzer, H. G. (2000). Determining glutathione and glutathione disulfide using the fluorescence probe o-phthalaldehyde. *Anal. Biochem.* **280,** 80–86.

Shen, D., Dalton, T. P., Nebert, D. W., and Shertzer, H. G. (2005). Glutathione redox state regulates mitochondrial reactive oxygen production. *J. Biol. Chem.* **280,** 25305–25312.

Shen, S., Wertheimer, E., Sampson, S. R., and Tennenbaum, T. (2000). Characterization of glucose transport system in keratinocytes: Insulin and IGF-1 differentially affect specific transporters. *J. Invest. Dermatol.* **115,** 949–954.

Shertzer, H. G., Genter, M. B., Shen, D., Nebert, D. W., Chen, Y., and Dalton, T. P. (2006). TCDD decreases ATP levels and increases reactive oxygen production through changes in mitochondrial F(0)F(1)-ATP synthase and ubiquinone. *Toxicol. Appl. Pharmacol.* **217,** 363–374.

Stohs, S. J. (1990). Oxidative stress induced by 2,3,7,8-tetrachlorodibenzo-p-dioxin (TCDD). *Free Radic. Biol. Med.* **9,** 79–90.

Suskind, R. R. (1985). Chloracne, "the hallmark of dioxin intoxication". *Scand. J. Work. Environ. Health* **11,** 165–171.

Sutter, C. H., Bodreddigari, S., Campion, C., Wible, R. S., and Sutter, T. R. (2011). 2,3,7,8-Tetrachlorodibenzo-p-dioxin increases the expression of genes in the human epidermal differentiation complex and accelerates epidermal barrier formation. *Toxicol. Sci.* **124,** 128–137.

Sutter, C. H., Bodreddigari, S., Sutter, T. R., Carlson, E. A., and Silkworth, J. B. (2010). Analysis of the CYP1A1 mRNA dose-response in human keratinocytes indicates that relative potencies of dioxins, furans, and PCBs are species and congener specific. *Toxicol. Sci.* **118,** 704–715.

Sutter, C. H., Yin, H., Li, Y., Mammen, J. S., Bodreddigari, S., Stevens, G., Cole, J. A., and Sutter, T. R. (2009). EGF receptor signaling blocks aryl hydrocarbon receptor-mediated transcription and cell differentiation in human epidermal keratinocytes. *Proc. Natl. Acad. Sci. U.S.A.* **106,** 4266–4271.

Sutter, T. R., Guzman, K., Dold, K. M., and Greenlee, W. F. (1991). Targets for dioxin: Genes for plasminogen activator inhibitor-2 and interleukin-1 beta. *Science* **254,** 415–418.

Tamiji, S., Beauvillain, J. C., Mortier, L., Jouy, N., Tual, M., Delaporte, E., Formstecher, P., Marchetti, P., and Polakowska, R. (2005). Induction of apoptosis-like mitochondrial impairment triggers antioxidant and Bcl-2-dependent keratinocyte differentiation. *J. Invest. Dermatol.* **125,** 647–658.

Tonack, S., Kind, K., Thompson, J. G., Wobus, A. M., Fischer, B., and Santos, A. N. (2007). Dioxin affects glucose transport via the arylhydrocarbon receptor signal cascade in pluripotent embryonic carcinoma cells. *Endocrinology* **148,** 5902–5912.

Tran, Q. T., Kennedy, L. H., Leon Carrion, S., Bodreddigari, S., Goodwin, S. B., Sutter, C. H., and Sutter, T. R. (2012). EGFR regulation of epidermal barrier function. *Physiol. Genomics* **44,** 455–469.

Uchida, Y., and Holleran, W. M. (2008). Omega-O-acylceramide, a lipid essential for mammalian survival. *J. Dermatol. Sci.* **51,** 77–87.